

**Behavior of bulky ferrofluids in the diluted low-coupling regime: Theory and simulation**Juan J. Cerdà,<sup>1</sup> Ekaterina Elfimova,<sup>2</sup> V. Ballenegger,<sup>3</sup> Ekaterina Krutikova,<sup>2</sup> Alexey Ivanov,<sup>2</sup> and Christian Holm<sup>1,4</sup><sup>1</sup>*Institute for Computational Physics, Universität Stuttgart, 70569 Stuttgart, Germany*<sup>2</sup>*Department of Mathematical Physics, The Urals State University, 51 Lenin Avenue, Ekaterinburg 620083, Russia*<sup>3</sup>*Institut UTINAM, Université de Franche-Comté, Route de Gray 16, 25030 Besancon, France*<sup>4</sup>*Max-Planck-Institut für Polymerforschung, Ackermannweg 10, D-55128 Mainz, Germany*

(Received 17 September 2009; revised manuscript received 8 December 2009; published 13 January 2010)

A theoretical formalism to predict the structure factors observed in dipolar soft-sphere fluids based on a virial expansion of the radial distribution function is presented. The theory is able to account for cases with and without externally applied magnetic fields. A thorough comparison of the theoretical results to molecular-dynamics simulations shows a good agreement between theory and numerical simulations when the fraction of particles involved in clustering is low; i.e., the dipolar coupling parameter is  $\lambda \leq 2$ , and the volume fraction is  $\varphi \leq 0.25$ . When magnetic fields are applied to the system, special attention is paid to the study of the anisotropy of the structure factor. The theory reasonably accounts for the structure factors when the Langevin parameter is smaller than 5.

DOI: [10.1103/PhysRevE.81.011501](https://doi.org/10.1103/PhysRevE.81.011501)

PACS number(s): 83.80.Gv, 47.65.Cb, 61.46.Df

**I. INTRODUCTION**

Ferrofluids are colloidal suspensions of ferromagnetic nanoparticles. The magnetic core of the particles is sufficiently small (typically 10–20 nm) for them to consist of magnetic monodomains characterized by a permanent dipole moment. The magnetic cores are usually stabilized against aggregation by steric coatings (in nonelectrolyte solutions) or by electrical double layers (in aqueous solutions). The changes in an external magnetic field of some of the properties of ferrofluids such as viscosity, phase behavior, or their optical birefringence make them useful in many areas, ranging from engineering, to biomedical applications, i.e., cancer treatment [1–5]. They are also of particular interest as models of dipolar fluids.

Despite the differences in sizes and magnetic materials that can be used to make ferrofluid particles [2,6], the behavior of a monodisperse ferrofluid system can be characterized by two dimensionless parameters: the volume fraction of particles  $\varphi = Nv_p/V$  (where  $N$  is the number of particles,  $v_p$  is the volume of a particle, and  $V$  is the total volume of the system), and the dipolar coupling parameter  $\lambda = 0.5U_{dd}/k_B T$ , where  $U_{dd}$  is the interaction energy of two particles in head-to-tail contact. When a uniform stationary magnetic field  $\mathbf{H}$  is introduced, a third dimensionless parameter, the Langevin parameter  $\alpha \equiv mH/(k_B T)$  (where  $m$  is the typical magnetic dipole of the particles) is needed to characterize the system. The use of  $\varphi$ ,  $\lambda$ , and  $\alpha$  allows a generalized description of ferrofluid systems.

Experiments [7–10], theories [11–23], and simulations [24–35] have shown that for values of  $\varphi$  and  $\lambda$  large enough, the ferrofluid particles tend to organize into many different types of aggregates, i.e., chains, rings, branched structures, and networks. For  $\lambda > 4$  and sufficiently large values of  $\varphi$  the formation of branched clusters and network aggregates is still poorly understood. The formation of aggregates as well as the related structure factors in three-dimensional systems in the regime  $\lambda \in (2, 4)$  has been studied recently using a new theoretical formalism that is capable to reproduce to a large extent the results observed in numerical simulations [36].

In the nonaggregating regime  $\lambda < 2$ , the physical properties of very diluted systems ( $\varphi \rightarrow 0$ ) are well described using the framework of the one-particle model [37], which treats the ferrofluid as an ideal paramagnetic gas of particles suspended in a liquid carrier. However, this model breaks down when either the particle concentration or the strength of the dipole-dipole interaction is increased.

Despite the fact that aggregates are negligible, correlations among particles exist. Several theoretical models have been proposed in order to explain the magnetic properties of nonaggregating ferrofluids which are based on adapted versions of the mean-field [38,39] and mean-spherical [40–45] models, as well as the thermodynamic perturbation model [46,47]. In this regime, structure factors determined experimentally are a valuable source of information [10,48–50], but it is difficult to extract from them a detailed knowledge about the correlations of the ferrofluid particles. Thus, theoretical methods that can relate the observed structure factors to the interparticle correlations in the ferrofluid are desirable. In order to explain the observed radial distribution functions and structure factors a theoretical framework has been recently proposed [51] for the case of dipolar hard spheres (DHS) at zero field in the low-coupling regime  $\lambda < 2$ . However, that model has not been stringently tested against numerical results.

In this paper we extend the previous approach [51] to the case of DHS in an externally applied magnetic field, and subsequently we also extend it to the case of dipolar soft spheres (DSS) ferrofluids in zero and nonzero fields. The interaction between DSS particles is modeled as the sum of two pairwise potentials: a soft-core plus a dipole-dipole interaction. The soft-core interaction is a cut-shifted Lennard-Jones potential [52], also called Weeks-Chandler-Andersen (WCA) potential [53], of the form

$$U_{ss}(r_{ij}) = \begin{cases} \varepsilon \left[ 1 - 2 \left( \frac{\sigma}{r_{ij}} \right)^6 \right]^2, & r_{ij} < 2^{1/6} \sigma \\ 0, & r_{ij} > 2^{1/6} \sigma, \end{cases} \quad (1)$$

where  $\sigma$  has the meaning of an effective ferroparticle diameter including steric shell, and the energy parameter  $\varepsilon$  describes the shell hardness,  $U_{ss}(r_{ij}=\sigma)=\varepsilon$ . The point dipole-dipole potential is

$$U_d(ij) = - \left[ 3 \frac{(\mathbf{m}_i \cdot \mathbf{r}_{ij})(\mathbf{m}_j \cdot \mathbf{r}_{ij})}{r_{ij}^5} - \frac{(\mathbf{m}_i \cdot \mathbf{m}_j)}{r_{ij}^3} \right], \quad \mathbf{r}_{ij} = \mathbf{r}_i - \mathbf{r}_j. \quad (2)$$

The latter is of noncentral character, since it depends not only on the interparticle distance  $r_{ij}$  but also on the mutual orientation of the magnetic moments of the two particles. In terms of the potential parameters, the dipolar coupling constant  $\lambda$  can be rewritten as  $\lambda = m^2 / \sigma^3 k_B T$ . The extension of the theory for DHS to DSS systems is done by using an effective hard-sphere diameter mapping. The predictions of the theoretical model are then thoroughly compared to the results of molecular-dynamics (MD) simulations. Special emphasis is given to the study of the anisotropy of the structure factor in the presence of magnetic fields.

The theory is presented in Sec. II. After a brief summary of the results already obtained for the DHS model (Sec. II A) at zero field, the theory is extended to the case of an externally applied magnetic field in Sec. II B and to the DSS model in Sec. II C. In Sec. III, details about the MD simulations for generating the test cases for the theoretical model are given. A stringent comparison between theory and simulation is presented in Sec. IV. Finally, the main conclusions are summarized in Sec. V.

## II. THEORETICAL MODEL

### A. DHS pair distribution function: Zero magnetic field

The simplest theoretical model for a ferrofluid consists of a system of monodisperse DHS with diameter  $d$  and constant magnetic moment  $m$ . The location of each  $i$ th particle and the orientation of its magnetic moment  $\mathbf{m}_i = m \boldsymbol{\Omega}_i$  are defined by the radius vector  $\mathbf{r}_i(r_i, \theta_i, \varphi_i)$  and by the vector  $\boldsymbol{\Omega}_i(\omega_i, \zeta_i)$ , where  $\omega_i$  is the zenith angle and  $\zeta_i$  is the azimuth angle of the orientation vector. The interparticle interaction energy  $U(ij)$  consists of two parts: the hard-sphere interaction

$$U_{hs}(r_{ij}) = \begin{cases} \infty, & 0 < r_{ij} < d \\ 0, & r_{ij} \geq d \end{cases} \quad (3)$$

and the dipole-dipole interaction given by Eq. (2).

Interparticle correlations are described by the pair distribution function  $g(\mathbf{r}_{ij}, \mathbf{m}_i, \mathbf{m}_j)$  which gives the probability density for the mutual position and orientations of two randomly chosen particles  $i$  and  $j$ . So, in general the DHS pair distribution function depends on the vector  $\mathbf{r}_{ij}$ , connecting the centers of these particles, and the magnetic moments of the particles,  $\mathbf{m}_i$  and  $\mathbf{m}_j$ . In the absence of an applied magnetic field the ferrofluid is isotropic, and the radial distribution function  $g(r_{ij})$ , averaged over all possible orientations of both magnetic moments, can be considered as

$$g(r_{ij}) \equiv \langle g(\mathbf{r}_{ij}, \mathbf{m}_i, \mathbf{m}_j) \rangle_{ij} \equiv \int d\boldsymbol{\Omega}_i \int d\boldsymbol{\Omega}_j g(\mathbf{r}_{ij}, \mathbf{m}_i, \mathbf{m}_j),$$

$$d\boldsymbol{\Omega}_i = (4\pi)^{-1} \sin \omega_i d\omega_i d\zeta_i. \quad (4)$$

It should be remarked that at high densities  $\rho\sigma^3 \approx 0.94$ , where  $\rho$  is the number density, strongly dipolar fluids of spherical particles have been predicted to exhibit a spontaneous long-ranged orientational order in the absence of an applied field [54,55]. Nonetheless, our assumption of an isotropic system in the absence of magnetic field can be considered adequate because we apply the theory to systems with much lower densities  $\rho\sigma^3 = 6\varphi/\pi < 0.48$ . To obtain the radial distribution function we use a virial expansion in terms of the ferroparticle volume concentration  $\varphi$  [56]:

$$g(r_{12}) = \left\langle \exp \left[ - \frac{U_{hs}(r_{12})}{k_B T} - \frac{U_d(12)}{k_B T} \right] \times \left[ 1 + \sum_{p=3}^{\infty} \beta_p(12) \varphi^{p-2} \right] \right\rangle_{12}. \quad (5)$$

The dominant Boltzmann term  $\exp[-U_{hs}(r_{12})/k_B T - U_d(12)/k_B T]$  takes into account only the direct correlations between two particles. Each coefficient  $\beta_p(12)$  describes the influence of other  $p-2$  particles on the probability density of the two first ones. These coefficients are defined by the  $p$ -particle cluster integrals based on a diagrammatic expansion method [56]:

$$\beta_p(12) = \frac{1}{(p-2)!} \int d\mathbf{r}_3 \dots d\mathbf{r}_p \int d\boldsymbol{\Omega}_3 \dots d\boldsymbol{\Omega}_p \sum_{\Delta} S_{\Delta} \left( \prod f_{kl} \right)_{\Delta},$$

$$d\mathbf{r}_i = r_i^2 dr_i \sin \theta_i d\theta_i d\varphi_i, \quad (6)$$

where  $S_{\Delta}$  are the number of diagrams with the same topology  $\Delta$ , and the Mayer functions  $f_{kl} = \exp[-U(kl)/k_B T] - 1$  depend on the interaction potential  $U(kl)$  between particles  $k$  and  $l$ . The integration over  $d\mathbf{r}_k$  corresponds to averaging over the position of the  $k$ th particle, and for each coefficient  $\beta_p(12)$  this averaging should be made over positions from the third to the  $p$ th particles.

For real ferrofluids with typical ferroparticle size  $d \sim 10$  nm the dipolar coupling constant is of the order of unity,  $\lambda \sim 1$ . In the low-coupling regime, it is reasonable to expand Eq. (5) in a power series over  $\lambda$ . At zero magnetic-field strength the averaging over the orientations of particle magnetic moments gives immediately

$$\langle U_d(ij) \rangle_{ij} = 0, \quad \langle U_d(ij) U_d(jk) \rangle_{ijk} = 0, \quad \langle U_d(ij) U_d(kl) \rangle_{ijkl} = 0,$$

$$\left\langle \left[ \frac{U_d(ij)}{k_B T} \right]^2 \right\rangle_{ij} = \frac{2\lambda^2}{3} \left( \frac{d}{r_{ij}} \right)^6.$$

Therefore, the nonvanishing contributions in Eq. (5) are of order  $\sim \lambda^2$ . Restricting our analysis to  $\lambda^2$  and  $\varphi^2$  terms in the virial series, we get for the orientation-averaged radial distribution function

$$g(r) = \exp\left[-\frac{U_{hs}(r)}{k_B T}\right] \left\{ \left(1 + \frac{\lambda^2}{3r^6}\right) [1 + h_{hs}(r, \varphi)] + \lambda^2 \varphi \beta_3^d(r) + \lambda^2 \varphi^2 \beta_4^d(r) \right\}. \quad (7)$$

From now on, distances are measured in units of the particle diameter:  $r = r_{12}/d$ . The expression  $[1 + h_{hs}(r, \varphi)]$  is the hard-sphere radial distribution function, which can be found, for instance, with the help of the Percus-Yevick approximation [56–58] or the virial expansion [59]. The functions  $\beta_p^d(r)$

take into account the dipole-dipole interparticle interaction, and the three- and four-particle contributions were first calculated in Ref. [51]:

$$\beta_3^d(r) = \frac{1}{3} \begin{cases} 0, & 0 < r < 1 \\ \frac{r(3r^3 + r^2 - 12r - 12)}{(r+1)^3}, & 1 \leq r < 2 \\ -\frac{16}{(r^2-1)^3}, & r \geq 2, \end{cases}$$

$$\beta_4^d(r) = \frac{1}{3} \begin{cases} 0, & 0 < r < 1 \\ 6 \ln \left[ \frac{(r+2)^3 r^2}{64(r+1)^2} \right] + \frac{1}{10r^2(r+2)(r+1)^3} (9r^{10} - 15r^9 - 219r^8 - 42r^7 + 1148r^6 + 1051r^5 - 555r^4 + 124r^3 + 1187r^2 + 162r - 240), & 1 \leq r < 2 \\ 6 \ln \left[ \frac{(r+2)^3}{4r^2(r+1)^2} \right] - \frac{1}{10r^2(r^2-1)^3(r+2)} (9r^{13} - 42r^{12} - 147r^{11} + 861r^{10} + 112r^9 - 4768r^8 + 2382r^7 + 9478r^6 - 6823r^5 - 8406r^4 + 7153r^3 + 5357r^2 - 366r + 240), & 2 \leq r < 3 \\ 6 \ln \left[ \frac{(r^2-4)^3}{r^2(r^2-1)^2} \right] + \frac{1}{r^2(r^2-4)(r^2-1)^3} (60r^8 - 282r^6 + 446r^4 - 152r^2 + 48), & r \geq 3. \end{cases} \quad (8)$$

Looking at the radial distribution function (7), we could say that the first terms are formed by the hard-sphere radial distribution function  $\exp[-U_{hs}(r)/k_B T][1 + h_{hs}(r, \varphi)]$  with additional short range influence of the dipolar factor  $\sim \lambda^2/r^6$ . The three-particle contribution  $\beta_3^d(r)$  results in the growth of first peak ( $r \gtrsim 1$ ) and the appearance of the first minimum ( $r \sim 1.5$ ). The four-particle term  $\beta_4^d(r)$  tends to further deepen this minimum and leads to the formation of a second maximum ( $r \sim 2$ ) in the second coordination sphere. Therefore, the short range ordering in dipolar fluids is governed by both the hard-sphere part and the dipole-dipole interaction.

### B. DHS pair distribution function: Nonzero magnetic field

Now let us consider the case of an externally applied magnetic field. Evidently, an applied field induces anisotropy in ferrofluid. We have chosen the shape of the ferrofluid container in such a way that the influence of the demagnetization field can be neglected, namely, we consider the shape of an infinitely elongated ellipsoid of revolution (the ratio of the minor to major ellipsoid semiaxis should tend to zero) stretched along an external uniform magnetic field  $\mathbf{H}$ . For this case the external magnetic field coincides exactly with the internal one, and the demagnetization factors do not need to be taken into account. We use a Cartesian  $(x, y, z)$  coordinate system with the  $z$  axis oriented parallel to the major axis of the ellipsoid, that is,  $\mathbf{H} \parallel Oz$ ; the angles  $\varphi_i, \zeta_i$  denote the azimuth angles in the plane  $(x, y)$ ; and the angles  $\theta_i, \omega_i$  are

the zenith angles between the vectors  $\mathbf{r}_i, \Omega_i$  and the  $z$  axis (direction  $\mathbf{H}$ ).

The magnetic field gives rise to a magnetic interaction energy  $U_m(i) = -(\mathbf{m}_i \cdot \mathbf{H})$ . Therefore, the averaging over the  $i$ th magnetic moment orientations should include the one-particle orientational distribution function:

$$\langle f(\Omega_i) \rangle_i = \frac{\alpha}{\sinh \alpha} \int d\Omega_i \exp(\alpha \cos \omega_i) f(\Omega_i), \quad (9)$$

where  $\alpha = mH/k_B T$  is the Langevin parameter and  $\alpha/\sinh(\alpha)$  is the normalization factor. The previous equation is in fact the definition of the averaging operator for an arbitrary function  $f(\Omega_i)$  in the presence of a field.

Due to the anisotropy, the radial distribution function (4) is no longer rotationally invariant and becomes dependent on the direction of the vector  $\mathbf{r}_{ij}$ . According to Eq. (9) the averaging of the dipole-dipole potential  $U_d$  over orientations of the magnetic moments gives a nonzero linear term in  $\lambda$ , which depends on the squared Langevin function  $L(\alpha) = \coth \alpha - 1/\alpha$ :

$$\left\langle -\frac{U_d(ij)}{k_B T} \right\rangle_{ij} = \lambda L^2(\alpha) (3 \cos^2 \theta_{ij} - 1) \left( \frac{d}{r_{ij}} \right)^3, \quad (10)$$

where  $\theta_{ij}$  is the angle between vector  $\mathbf{r}_{ij}$  and the direction of the magnetic field  $\mathbf{H}$ . At low and moderate magnetic fields this linear term is the dominant contribution to the pair distribution function, and we do not consider the quadratic

terms in  $\lambda$ . As a result the pair distribution function is proportional to  $\sim L^2(\alpha)$ :

$$g(r, \theta) = \exp\left[-\frac{U_{hs}(r)}{k_B T}\right] \left[ \left( 1 + \lambda L^2(\alpha) \frac{3 \cos^2 \theta - 1}{r^3} + \frac{\lambda^2}{3r^6} \right) \times [1 + h_{hs}(r, \varphi)] + \lambda \varphi L^2(\alpha) \frac{3 \cos^2 \theta - 1}{r^3} \beta_3^{df}(r) + \lambda^2 \varphi \beta_3^d(r) + \lambda^2 \varphi^2 \beta_4^d(r) \right], \quad \theta \equiv \theta_{12}, \quad (11)$$

where the function  $\beta_3^{df}(r)$  is calculated in the same way as in zero-field case (6) by averaging over all positions and orientations of the third particle in a field [60]:

$$\beta_3^{df}(r) = \begin{cases} 0, & 0 < r < 1 \\ -3r^4 + r^6/2, & 1 \leq r < 2 \\ -16, & r \geq 2, \end{cases} \quad (12)$$

where the superscript *df* stands for ‘‘dipoles in a field.’’ Hence, in the framework of the considered approximation the anisotropy of the pair distribution function is described by the second Legendre polynomial over  $\theta$ . Moreover, these contributions are long ranged and decay rather slowly ( $\sim 1/r^3$ ).

The field-induced anisotropy of the DHS pair distribution function is presented in Fig. 1. Plots (a)–(c) correspond to the case  $\lambda=1$  and  $\varphi=0.1$ , whereas plots (d)–(f) correspond to the same  $\lambda$  value but  $\varphi=0.2$ . Plots (a) and (d) correspond to the case of zero field. Here, pair distribution function (11) coincides with expression (7) and is isotropic. The bright white shell describes the first peak; the next dark region shows the first minimum. A weak pronounced second maximum can also be observed for the chosen volume concentration of 20% (the outermost bright region). Even a weak magnetic field [ $\alpha=1$ ; plots (b) and (e)] leads to a drastic change in the DHS microstructure. Along the magnetic-field direction the first minimum becomes deeper and wider, while the second maximum becomes more pronounced perpendicular to the magnetic-field direction. The latter effect is obvious, since for the perpendicular direction the dipole-dipole interaction is repulsive. Thus, a second particle is located at some distance away from the first one with higher probability than at close contact. This behavior is more pronounced with high field strength [ $\alpha=5$ ; plots (c) and (f)]. The probability of the ‘‘head-to-tail’’ contact is quite high, and we observe a trend of forming ferroparticle dimers. For larger concentrations and larger dipolar forces a second maximum in parallel direction also appears.

### C. DSS pair distribution function

In our MD simulations the ferrofluid is modeled as a system of DSS. The theory developed above can be easily adapted to this case in the following way: in Eq. (11) the hard-sphere potential  $U_{hs}$  in the Boltzmann term is substituted by the soft-sphere potential  $U_{ss}$ . This potential energy of contacting soft spheres can be modeled, for example, by a Yukawa potential (for ionic stabilized ferrofluids) or other short range repulsions for ferrofluids with sterical stabiliza-

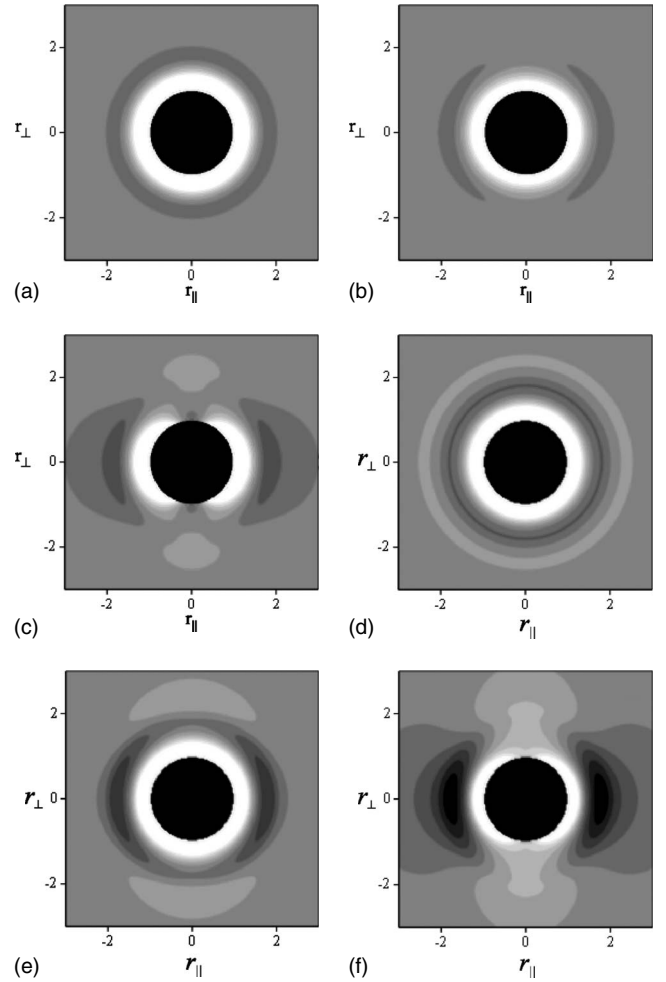


FIG. 1. Anisotropy of the pair distribution function in a magnetic field. The contour plots are presented for function (11) in the plane  $Or_{\parallel}r_{\perp}$ , where  $r_{\parallel}$  and  $r_{\perp}$  are the radius-vector components, parallel and perpendicular to the magnetic-field direction. The dipolar coupling constant is chosen as  $\lambda=1$ , and the volume fraction is  $\varphi=0.1$  for plots (a)–(c), and  $\varphi=0.2$  for plots (d)–(f). The values of the dimensionless magnetic field are  $\alpha=0$  for plots (a) and (d),  $\alpha=1$  for plots (b) and (e), and  $\alpha=5$  for plots (c) and (f).

tion. Here we use the WCA potential given by Eq. (1).

All multiparticle contributions are calculated in the same way as for expression (11) using an effective hard-sphere diameter  $d_e$ :

$$d_e = \int_0^{\infty} \left[ 1 - \exp\left(-\frac{U_{ss}}{k_B T}\right) \right] dr. \quad (13)$$

The effective repulsive energy is set equal to the thermal energy during the simulations, that is,  $\varepsilon=k_B T$ . This yields an effective hard-sphere diameter  $d_e$  quite close to  $\sigma:d_e = 1.016\sigma$ .

The structure factor is obtained from  $g(\mathbf{r})$  via a Fourier transform,

$$S(\mathbf{q}) = 1 + n \int d\mathbf{r} e^{-i\mathbf{q}\cdot\mathbf{r}} [g(\mathbf{r}) - 1], \quad (14)$$

where  $n$  is the ferroparticle number density, and  $\mathbf{q}$  is the scattering wave vector.

### III. SIMULATION MODEL

We model the ferrofluids in our equilibrium MD simulations as systems consisting of  $N$  spherical particles of diameter  $\sigma$ , distributed in a cubic simulation box of side length  $L$ . Similarly to the theory, we assume particles to be monodisperse and exhibit a permanent point dipole moment  $\mathbf{m}$  at its center, which can freely rotate in 3D. The interaction energy between two particles is the sum of the short range interaction Eq. (1) and the dipolar interaction Eq. (2). Periodic boundary conditions are assumed along all directions. The long-range dipole-dipole interactions are calculated using a recently developed dipolar  $\mathbf{P}^3\mathbf{M}$  algorithm [61]. The use of the dipolar  $\mathbf{P}^3\mathbf{M}$  method allows a much faster calculation of the dipolar long-range correlations than the traditional three-dimensional dipolar Ewald summation. The level of accuracy of the algorithm for computing dipolar forces and torques is set to  $\delta \sim 10^{-4}$  in reduced units of force  $f^* = f\sigma/\varepsilon$  and torque  $\tau^* = \tau/\varepsilon$ .

In the simulations, the particles move according to the translational and rotational Langevin equations of motion which read for particle  $i$  [62]

$$M_i \frac{d\mathbf{v}_i}{dt} = \mathbf{F}_i - \Gamma_T \mathbf{v}_i + \boldsymbol{\xi}_i^T, \quad (15)$$

$$\mathbf{I}_i \cdot \frac{d\boldsymbol{\omega}_i}{dt} = \boldsymbol{\tau}_i + \mathbf{m} \times \mathbf{H} - \Gamma_R \boldsymbol{\omega}_i + \boldsymbol{\xi}_i^R, \quad (16)$$

where  $\mathbf{F}_i$ ,  $\boldsymbol{\tau}_i$ , and  $\mathbf{H}$  are the resulting force, torque, and the external magnetic field acting on the particle  $i$ , respectively.  $M_i$  and  $\mathbf{I}_i$  are the mass and the inertia tensor of the particle. The symbols  $\Gamma_T$  and  $\Gamma_R$  stand for the translational and rotational friction constants, respectively.  $\boldsymbol{\xi}_i^T$  and  $\boldsymbol{\xi}_i^R$  are Gaussian distributed random forces and torques with zero mean that satisfy the usual fluctuation-dissipation relations. The variables can be given in dimensionless form as length  $r^* = r/\sigma$ , dipole moment  $(m^*)^2 = m^2/(\varepsilon/\sigma^3)$ , time  $t^* = t[\varepsilon/(M\sigma^2)]^{1/2}$ , temperature  $T^* = k_B T/\varepsilon$ , and external magnetic field  $H^* = H(\sigma^3/\varepsilon)^{1/2}$ . The simulations are performed at constant temperature  $T^* = 1$ . Since we are only interested in static observables, the values of the mass, the inertia tensor, as well as friction constants  $\Gamma_T$  and  $\Gamma_R$  are somewhat at our disposal. The particle mass is chosen to be  $M = 1$ , and the inertia tensor  $\mathbf{I} = \mathbf{1}$ , the identity matrix, to ensure isotropic rotations. We adopted  $\Gamma_T = 1$ , and  $\Gamma_R = 3/4$  which are observed in our systems to give a fast relaxation toward the equilibrium. A reduced time step  $\Delta t^* \sim 15 \times 10^{-4}$  is used. The runs are started from initial configurations with random particle positions distributed over the simulation volume and randomly chosen orientations for the dipole moments of the particles. Each system is first equilibrated for a period of  $7 \times 10^5$  time steps to ensure that the results are independent of the starting con-

ditions. In order to read a proper and almost uncorrelated sampling, measures are taken at intervals of  $15 \times 10^3 \Delta t^*$  for another period of  $2 \times 10^6$  time steps. The number of particles per system is  $N = 1000$  in regular simulations, although several extra runs (up to  $N = 10\,000$ ) have been performed in order to make sure results do not suffer from finite-size effects. The simulation package ESPRESSO [63] has been used to perform the simulations.

### IV. RESULTS

In this section we compare the theoretical predictions against the results from our MD simulations. For the sake of clarity, the results are presented in two subsections: one for the systems without magnetic field and one for systems with an externally applied magnetic field in the  $z$  direction. As pointed out in the introduction, the structure  $S(\mathbf{q})$  factor plays a main role in the characterization of a physical system. Once the structure factor of a system is known, many other important observables can be derived from it.

As in our previous numerical study [31], we compute the structure factor as

$$S(\mathbf{q}) = \frac{1}{N} \left\langle \left[ \sum_{i=1}^N \sin(\mathbf{q} \cdot \mathbf{r}_i) \right]^2 + \left[ \sum_{j=1}^N \cos(\mathbf{q} \cdot \mathbf{r}_j) \right]^2 \right\rangle, \quad (17)$$

where the wave vectors  $\mathbf{q}$  have to be commensurate with the periodic boundary conditions, i.e.,  $\mathbf{q} \equiv (q_x, q_y, q_z) = (2\pi/L)(l, m, n) \neq (0, 0, 0)$ , where  $l$ ,  $m$ , and  $n$  are integers. For systems without an applied magnetic field, the fluid structure is rotationally invariant, and a spherically averaged structure factor  $S(q)$ , obtained by averaging over all wave vectors of magnitude  $q = |\mathbf{q}|$ , is enough to characterize these systems. For the systems with a magnetic field applied along the  $z$  direction,  $S(\mathbf{q})$  is anisotropic. Nonetheless, it has been shown in previous studies [10,31,64] that it is enough to characterize those systems two different structure factors: one parallel to the magnetic field  $S(q_{\parallel})$  and one perpendicular to the magnetic field  $S(q_{\perp})$ , namely,

$$S(q_{\parallel}) = \frac{1}{N} \left\langle \left[ \sum_{i=1}^N \sin(q_{\parallel} z_i) \right]^2 + \left[ \sum_{j=1}^N \cos(q_{\parallel} z_j) \right]^2 \right\rangle, \quad (18)$$

$$S(q_{\perp}) = \frac{1}{N} \left\langle \left[ \sum_{i=1}^N \sin(\mathbf{q}_{\perp} \cdot \mathbf{r}_{xy,i}) \right]^2 + \left[ \sum_{j=1}^N \cos(\mathbf{q}_{\perp} \cdot \mathbf{r}_{xy,j}) \right]^2 \right\rangle, \quad (19)$$

where  $q_{\parallel} \equiv q_z = (2\pi/L)n$ ,  $\mathbf{q}_{\perp} \equiv (q_x, q_y, 0) = (2\pi/L)(l, m, 0)$ , and  $\mathbf{r}_{xy,i} = (x_i, y_i, 0)$ . The rotational symmetry of the system along the  $z$  axis allows us to average the perpendicular structure factor as  $S(q_{\perp})$  where  $q_{\perp} = |\mathbf{q}_{\perp}| = \sqrt{q_x^2 + q_y^2}$ .

The approximations leading to Eq. (7) are justified, as long as the correlations between the dipolar particles are weak. Once they start to aggregate, forming chains, rings, and other branched structures [23,35], we expect the theoretical description to break down. Figure 2 shows the dependence of the fraction of particles not involved in clusters, at

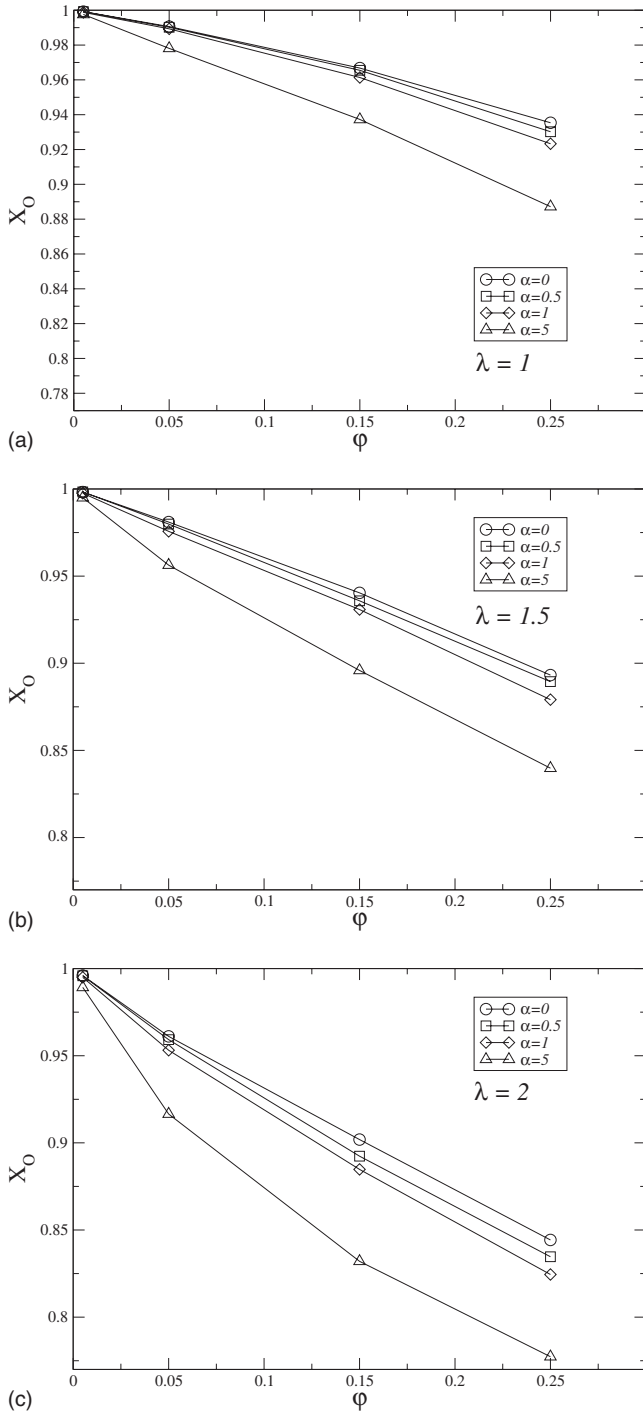


FIG. 2. Simulation results for the fraction of particles in the system that is not forming clusters. We use the energy criteria at 70%; i.e., if the dipolar energy between two particles is larger than 70% of the maximum energy two particles can have at a distance equal to the diameter of one particle, then we say that the particles are linked and form a cluster. Plots (a), (b), and (c) show results for  $\lambda=1, 1.5,$  and  $2,$  respectively. Different intensities of external magnetic field are shown ranging from zero  $\alpha=0$  up to a value of the Langevin parameter (see text) of  $\alpha=5$ . As one would expect, by increasing either the dipolar coupling  $\lambda$  or the magnetic field  $\alpha$  the number of “free” particles decreases. In the most unfavorable case, around 22% of particles participate in the formation of clusters.

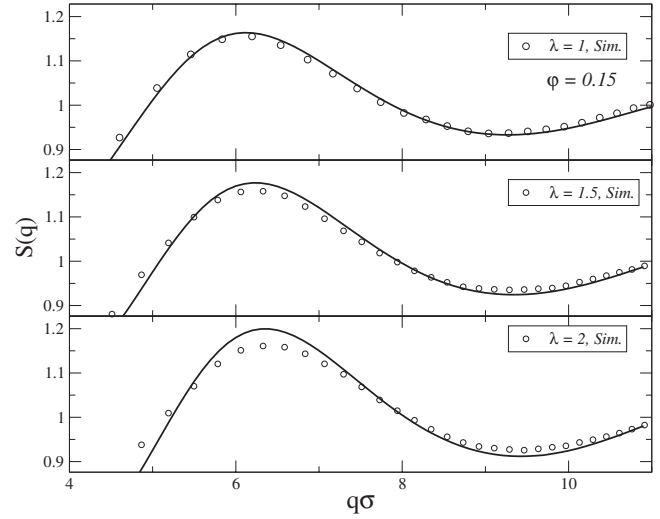


FIG. 3. A comparison of the structure factor data obtained at  $\varphi=0.15$  with no applied field, one from the simulations (circles) and one from the analytical theory (solid line). The value of  $\lambda$  changes from top to bottom from  $\lambda=1,$  to  $\lambda=1.5,$  and  $\lambda=2.$

volume fraction  $\varphi$  and dipolar coupling parameter  $\lambda,$  for several intensities of the magnetic field  $\alpha.$  Clusters are defined on the basis of an energy criteria [26]: two particles are considered to belong to a same cluster if their interacting energy is smaller than 70% of the minimum energy that occurs when both particles are separated by a distance  $\sigma$  and the dipoles are parallel; i.e., they are linked if  $U < 0.7U_{\min}$  where  $U_{\min} = -2m^2/\sigma^3.$  Different values of  $\lambda=1, 1.5, 2,$  and volume fraction  $\varphi=0.005, 0.05, 0.15,$  and  $0.25$  are studied. As expected, Fig. 2 shows that in increasing either  $\lambda$  or  $\varphi$  the number of free particles reduces, although the fraction of particles involved in clusters never exceed the 15% in the case of non-magnetic field  $\alpha=0.$  It is therefore advisable to take into account only systems with dipolar coupling parameter  $\lambda \leq 2$  and volume fractions smaller than  $\varphi \leq 0.25$  in our comparison.

**A. Systems without an externally applied magnetic field**

Figures 3 and 4 show the comparison of the isotropic structure factor  $S(q)$  between theory (lines) and the numerical simulations (open circles) for different values of the dipolar coupling parameter  $\lambda=1, 1.5,$  and  $2$  at fixed volume fractions  $\varphi=0.15$  and  $\varphi=0.25,$  respectively. A good agreement between theoretical predictions and simulation results is observed for wave vectors  $q\sigma > 3$  in the case of  $\lambda=1$  and  $q\sigma > 6$  for  $\lambda=1.5, 2.$

For lower values of  $q$  spurious peaks in the theoretical predictions are observed, especially at high values of  $\lambda.$  We attribute this to the fact that at low wave vectors the structure factor is sensitive to long-range many-body effects, while the present theory is limited to four-body effects. To get the correct behavior at low wave vectors, more terms need to be added to the virial expansion in powers of  $\varphi$  [Eqs. (7) and (11)] to take into account that the dipole-dipole interaction dominates over the hard-sphere part. When  $\lambda \ll 1$  the expected monotonic behavior of a hard-sphere system is recov-

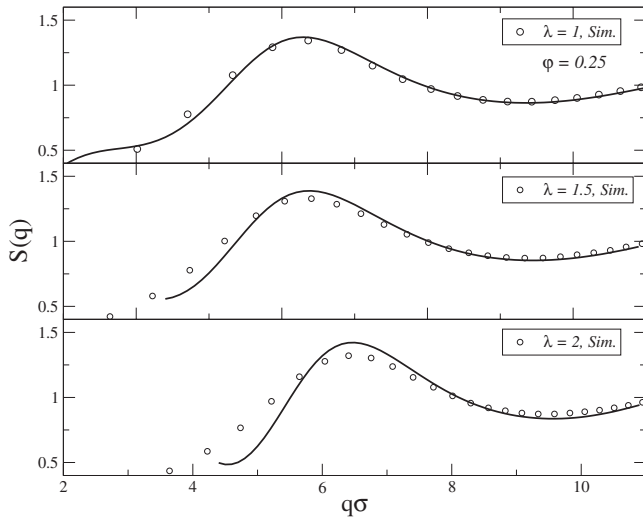


FIG. 4. Same as in Fig. 3 but for volume fraction  $\varphi = 0.25$ .

ered at low wave vectors. The calculation of the five-particle contribution  $\beta_5^d(r)$  and higher orders is mathematically quite involved and it will be aimed at in a subsequent work.

The mismatch between theory and simulations increases with  $\lambda$ . This is expected to occur due to the increase in the number of particles involved in the formation of clusters; see Fig. 2. Figures 3 and 4 clearly show that the upper boundary of the model lies around  $\lambda \sim 2$ . Remarkably the rod model developed by Pyanzina *et al.* [36] has been observed to describe quite accurately the structure factors obtained in MD simulations for values of  $\lambda$  in the range 2–5. Unfortunately this model cannot be applied to the nonaggregate regime  $\lambda < 2$  because the Pyanzina approach assumes the existence of aggregates larger than one particle in the system. We should stress at this point that the Pyanzina model and the theory we propose are complementary. With the help of both models, it is possible to predict the structure factors in ferrofluids up to the point where the formation of branched structures plays a dominant role (which typically occurs for  $\lambda > 5$ ). Therefore, the combination of both models allows the description of real ferrofluid systems on a broad parameter regime.

When the volume fraction  $\varphi$  increases (at constant  $\lambda$ ), the mean distance among particles reduces and correlations become stronger. This effect can be observed by comparing in Figs. 5 and 6 the height of peaks which are higher at larger volume fractions. Figure 5 depicts the position of the first physical maximum  $q_{\max}\sigma$  as a function of the volume fraction  $\varphi$  for different values of the dipolar coupling parameter  $\lambda$ . A clear shift toward larger wave vectors  $q$  is observed in Fig. 6 at larger volume fractions  $\varphi$ , which points to the fact that correlation between particles occurs at shorter distances. In addition, Fig. 6 shows that at constant volume fraction there is a shift toward larger wave vectors when the coupling parameter  $\lambda$  increases. The behavior observed in Fig. 6, in our opinion, is compatible with the fact that the radial distribution function  $g(r)$  is known to be an expansion in powers of the concentration  $\varphi$ , and  $S(q)$  is linked to  $g(r)$  via Eq. (14). Thus, at low concentration values, one expects the linear term with  $\varphi$  to dominate, and  $q_{\max}$  should exhibit a linear behavior with  $\varphi$ .

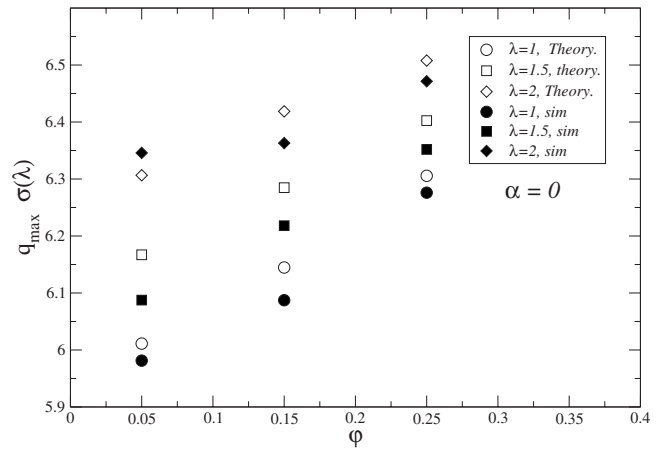


FIG. 5. A comparison between theory and simulations for the value of  $q\sigma$  at which the main peak in the structure factor occurs as a function of the volume fraction  $\varphi$ . The comparison is done for  $\lambda = 1, 1.5, \text{ and } 2$  at zero field  $\alpha = 0$ .

It could be tempting to try to relate the existence of the first peak of  $S(q)$  to the formation of cluster structures: in Fig. 2, it has been shown that the percentage of particles involved in clusters increases with  $\lambda$  and therefore it could significantly modify the structure factor even at  $\lambda < 2$ . But this last argument seems to be in contradiction with the observation that at fixed volume fraction (i.e., similar free mean distance between particles) the height of the peaks remains roughly the same as observed in Figs. 3 and 4. If clusters were playing a dominant role, one should expect significant changes in the height of the structure factors when  $\lambda$  is increased. Thus, one should rule out the possibility that the shape of the structure factors is dominated by a few clusters in the system. Instead, the observed structure factors are mainly due to the correlations between particles which do *not* aggregate. Thus, when dealing with structure factors, one must be cautious doing a straight identification of the peaks with chains or other types of clusters.

### B. Systems with an externally applied magnetic field

The introduction of an external magnetic field can trigger the formation of chain aggregates [31]. Such aggregates represent strong correlations among particles that the present theory cannot take into account because we neglect them when we truncate the virial expansion. A rough estimate of the range of validity of the theory when external magnetic fields are applied can be obtained from Fig. 2. Imposed fields should not exceed Langevin parameters beyond  $\alpha \sim 5$  because for larger values the fraction of particles involved in clusters is significant. Langevin parameters ( $\alpha = 0.5, 1, 5$ ) are considered to benchmark the theory in the three different regimes where the magnetic-field effects are *smaller*, *similar*, and *stronger* than thermal effects. Similar values for parameters  $\lambda$  and  $\varphi$  as in Sec. IV A are considered.

The external magnetic field is imposed along the  $z$  direction, and therefore an anisotropic behavior of the structure factors  $S(\mathbf{q})$  is expected along this direction. For this reason we study both the parallel  $S(q_{\parallel})$  and the perpendicular  $S(q_{\perp})$

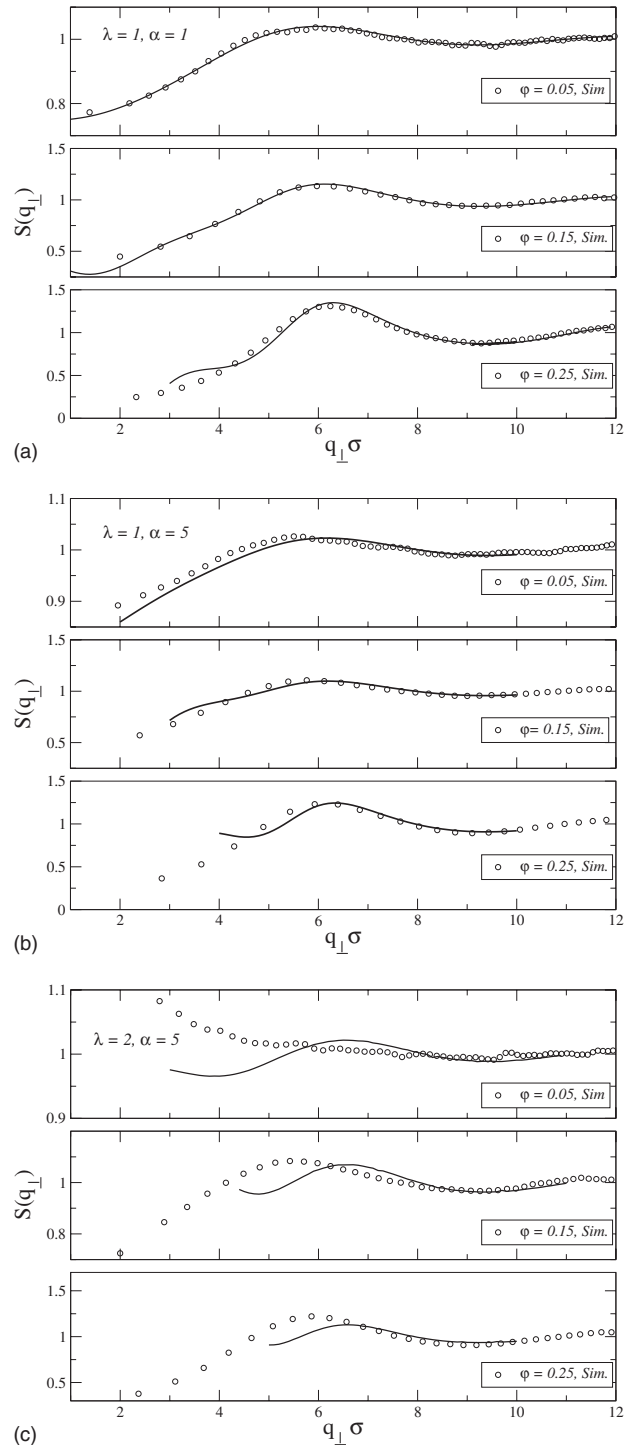
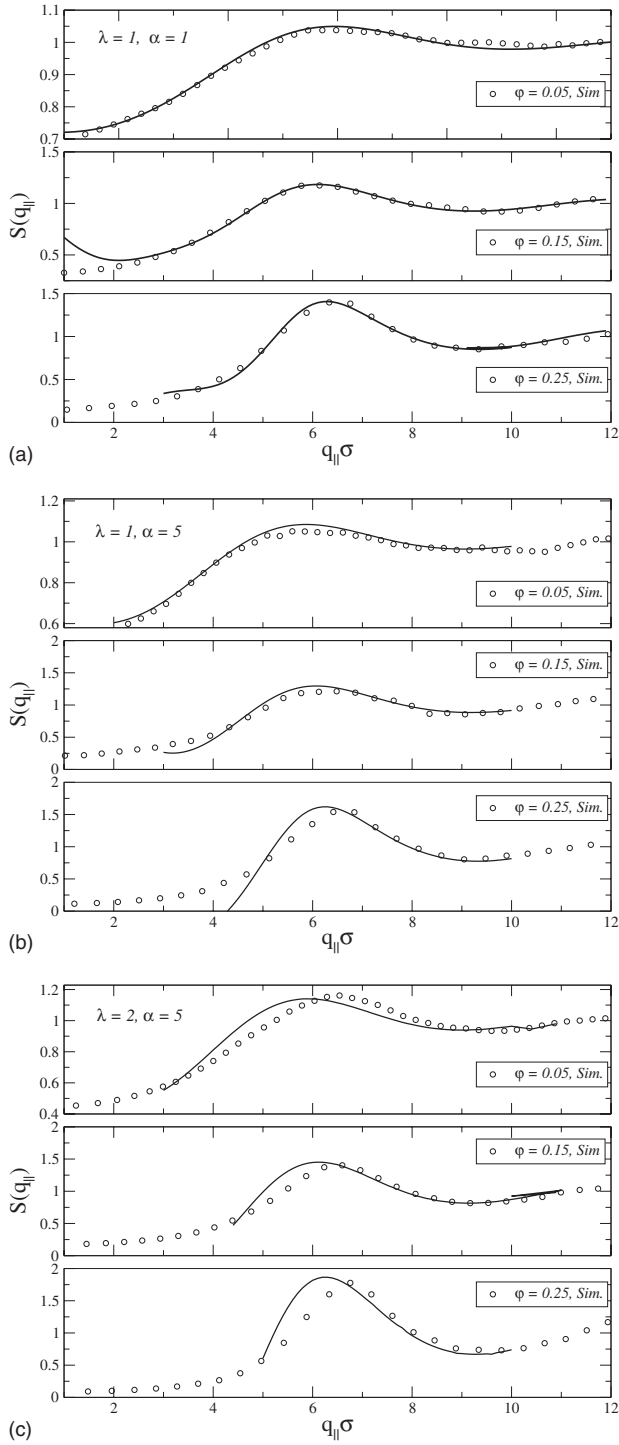


FIG. 6. A comparison of the structure factors parallel to the field predicted by the theory and those obtained in numerical simulations is depicted for several volume fractions  $\phi=0.05, 0.15,$  and  $0.25$  at different strengths of the magnetic field  $\alpha$  and dipolar coupling parameter  $\lambda$ . Plot (a) is for  $\lambda=1$  and Langevin parameter  $\alpha=1$ ; (b) is for  $\lambda=1$  and  $\alpha=5$ ; (c) is for  $\lambda=2$  and  $\alpha=5$ .

FIG. 7. Same as in Fig. 6 but for the component of the structure factor perpendicular to the magnetic field.

structure factors to the direction of the magnetic field which have been computed using Eq. (18).

Figures 6 and 7 show a comparison of the structure factors parallel  $S(q_{\parallel})$  and perpendicular  $S(q_{\perp})$  to the magnetic-field direction for several values of the area fraction  $\phi$ , the

dipolar coupling parameter  $\lambda$ , and the relative strength of the magnetic field  $\alpha$ . The theoretical and numerical structure factors parallel to the magnetic field show a reasonable agreement for  $\lambda=1$  and  $\alpha < 5$ . The worst results are observed in the case  $\lambda=2$  and  $\alpha=5$  where the number of particles expected to be involved in clusters is quite substantial and therefore the qualitative matching with the numerical simulations is partially lost. Nonetheless, it should be stressed that even for these high values of  $\alpha$  and  $\lambda$ , the theory still pro-

vides a significant physical insight about the structure factor parallel to the external magnetic field [see Fig. 6(c)].

For the case of the perpendicular component of the structure factor, see Fig. 6(a), the theory describes very well the behavior for  $\lambda=1$  and  $\alpha=1$ . The description is also adequate for  $\lambda=1$  and  $\alpha=5$  although at high densities only the behavior for long wave vectors is correctly depicted by the theory. In the case of  $\lambda=2$  and  $\alpha=5$  the theory fails to provide an adequate description of the structure factor. When comparing Figs. 6(c) and 7(c), it is observed that at large values of the dipolar coupling and magnetic field the parallel component of the structure factor is better described by the theory than the perpendicular component. This behavior might be caused by the influence of the triangle (three-particle) diagram: the three-particle term proportional to  $\lambda^3$  which is the leading contribution of the nonincluded terms in Eq. (7). We argue that three-particle effects are less important in parallel direction to the field because the main contribution comes from conformations close to the parallel alignment of the three particles head-to-tail along the field, which roughly is similar to the interaction of two dimers. On the other hand, in the perpendicular direction, the main contribution comes from conformations close to having two particles aligned along the field while the third dipole is perpendicular to it. That third dipole strongly interacts with the other two simultaneously, and therefore, in the perpendicular case, the neglected three-particle term is expected to be larger than in the parallel case.

As in the case of zero magnetic field (see Sec. IV A), the position of the first peak in the parallel and perpendicular components of the structure factor [ $S(q_{\parallel})$  and  $S(q_{\perp})$ ] moves toward large wave vectors and its height increases when the volume fraction  $\varphi$  is increased keeping  $\lambda$  and  $\alpha$  constant. These results can be explained in a similar way as for the non-magnetic-field case: more particles imply shorter distances among them and stronger correlations. On the other hand, the behavior of the two components is different when the dipolar coupling parameter  $\lambda$  is increased, keeping  $\alpha$  and  $\varphi$  constant. In the parallel component the first peak moves toward large wave vectors and its height increases when  $\lambda$  increases. For the perpendicular component the behavior is the inverse: when  $\lambda$  increases, the peaks reduce their height and the wave vectors are shifted toward lower values. This behavior comes from the fact that in the presence of a magnetic field, when  $\lambda$  increases, the particles increase their correlations along the direction of the magnetic field while the correlations are weakened along the perpendicular direction.

Figure 8 shows a comparison of the changes in the shape of the perpendicular structure factor when  $\lambda$  is increased for different values of the strength of the magnetic field and the volume fraction  $\varphi$ . As the different plots in Fig. 8 depict, the behavior of the perpendicular component of the structure factor at low volume fractions  $\varphi=0.05$  is very different from that observed at higher volume fractions  $\varphi=0.25$ . The differences in shape are even more notable when the strength of the magnetic field is increased. Figure 8(b) shows that the slope of the structure factor at low wave vectors changes gradually from positive to negative when the dipolar coupling  $\lambda$  increases. A similar trend can be observed in plot 8(a) although it is less pronounced. Nonetheless, the behav-

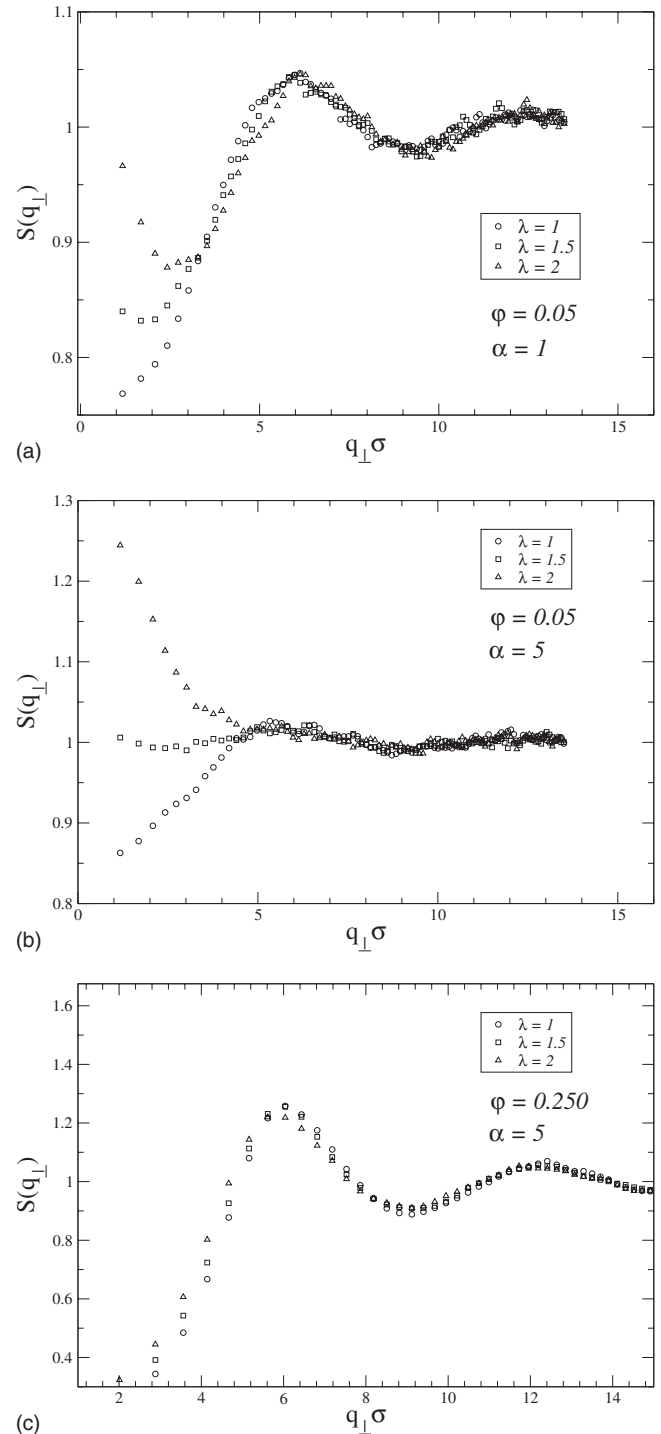


FIG. 8. The perpendicular structure factor in the presence of a magnetic field for different values of the dipolar coupling parameter  $\lambda=1, 1.5,$  and  $2$  at several volume fractions and magnetic-field values: in plot (a)  $\varphi=0.05$  and  $\alpha=1$ ; in plot (b)  $\varphi=0.05$  and  $\alpha=5$ ; in plot (c)  $\varphi=0.250$  and  $\alpha=5$ .

ior seems to be different at higher volume fractions as demonstrated in plot 8(c). At low volume fractions some long-range correlation seems to exist along the perpendicular direction that is induced by the magnetic field.

## V. CONCLUSIONS

In this work we have presented a theoretical framework to predict the structure factors observed in dipolar soft-sphere fluids when the aggregation among particles can be neglected. The comparison of the theory against MD simulations here shows that a good agreement between theory and numerical simulations can be observed when the fraction of particles involved in clustering is low, i.e., for small values of the dipolar coupling constant  $\lambda \lesssim 2$ , and small volume fractions  $\varphi \lesssim 0.25$ . In the case that external magnetic fields are present, the theoretical predictions show again remarkable agreement with simulation results for Langevin parameters  $\alpha < 5$ . Below these bounds, for  $q$  vectors  $q > 3$  the theory is able to provide an almost quantitative description of the structure factors. The analysis of the position of the peak maximum positions shows that in both theory and simulations, a shift toward higher wave vectors is expected when

either  $\lambda$  or the volume fraction  $\varphi$  is increased. In the regime of validity of the theory, in addition to the prediction of the structure factors and hence of the pair distribution function, it can be used to account for the behavior of associated observables such as pressure, free energy, heat capacity, chemical potential, as well as other thermodynamic functions.

We regard the present theory as complementary to the rod model developed by Pyanzina *et al.* [36] because it covers the region of low values of the dipolar coupling parameter  $\lambda$  where the Pyanzina model is not valid. The combined use of both theories leads to an accurate description of the structure factor for a broad range of dipolar soft-sphere systems.

## ACKNOWLEDGMENTS

This research has been carried out within the financial support of RFBR Grant No. 08-02-00647 and DFG-RFBR Joint Grants No. HO 1108/12-1 and No. 06-02-04019.

- 
- [1] R. E. Rosensweig, *Ferrohydrodynamics* (Cambridge University Press, Cambridge, 1985).
- [2] *Ferrofluids, Magnetically Controllable Fluids and Their Applications*, Lecture Notes in Physics, edited by S. Odenbach (Springer, New York, 2002).
- [3] C. Alexiou, R. Jurgons, R. J. Schmid, C. Bergmann, J. Henke, E. Huenges, and F. Parak, *J. Drug Target.* **11**, 139 (2003).
- [4] I. Hilger, W. Andrä, R. Hergt, R. Hiergeist, and W. A. Kaiser, in *Inorganic Materials, Recent Advances*, edited by D. Bahadur, S. Vitta, and O. Prakash (Narosa Publishing House, New Delhi, 2004).
- [5] C. Scherer and A. M. Figueiredo, *Braz. J. Phys.* **35**, 718 (2005).
- [6] C. Holm and J.-J. Weis, *Curr. Opin. Colloid Interface Sci.* **10**, 133, (2005).
- [7] L. Shen, A. Stachowiak, S. K. Fateen, P. E. Laibinis, and T. A. Hatton, *Langmuir* **17**, 288 (2001).
- [8] S. Odenbach, *Magnetoviscous Effects in Ferrofluids*, Springer Lecture Notes in Physics (Springer, Berlin, 2002).
- [9] M. Klokkenburg, R. P. A. Dullens, W. K. Kegel, B. H. Erne, and A. P. Philipse, *Phys. Rev. Lett.* **96**, 037203 (2006).
- [10] F. Gazeau, E. Dubois, J. C. Bacri, F. Boue, A. Cebers, and R. Perzynski, *Phys. Rev. E* **65**, 031403 (2002).
- [11] P. G. de Gennes and P. A. Pincus, *Z. Phys. B: Condens. Matter* **11**, 189 (1970).
- [12] P. C. Jordan, *Mol. Phys.* **25**, 961 (1973).
- [13] K. Sano and M. Doi, *J. Phys. Soc. Jpn.* **52**, 2810 (1983).
- [14] A. Y. Zubarev and L. Y. Iskakova, *J. Exp. Theor. Phys.* **80**, 857, (1995).
- [15] M. A. Osipov, P. I. C. Teixeira, and M. M. Telo da Gama, *Phys. Rev. E* **54**, 2597 (1996).
- [16] K. I. Morozov and M. I. Shliomis, *Ferrofluids, Magnetically Controllable Fluids and Their Application*, Springer Lecture Notes in Physics (Springer, Berlin, 2002), p. 162.
- [17] A. Yu. Zubarev, *Ferrofluids, Magnetically Controllable Fluids and Their Application*, Springer Lecture Notes in Physics (Springer, Berlin, 2002), p. 143.
- [18] A. O. Ivanov and S. S. Kantorovich, *Phys. Rev. E* **70**, 021401 (2004).
- [19] V. S. Mendeleev and A. O. Ivanov, *Phys. Rev. E* **70**, 051502 (2004).
- [20] E. Elfimova, A. O. Ivanov, and A. Yu. Zubarev, *Phys. Rev. E* **74**, 021408 (2006).
- [21] A. O. Ivanov, S. S. Kantorovich, V. S. Mendeleev, and E. S. Pyanzina, *J. Magn. Magn. Mater.* **300**, e206 (2006).
- [22] C. Holm, A. Ivanov, S. Kantorovich, E. Pyanzina, and E. Reznikov, *J. Phys.: Condens. Matter* **18**, S2737 (2006).
- [23] S. Kantorovich, J. J. Cerdà, and C. Holm, *Phys. Chem. Chem. Phys.* **10**, 1883 (2008).
- [24] E. Lomba, F. Lado, and J. J. Weis, *Phys. Rev. E* **61**, 3838 (2000).
- [25] J. J. Weis, J. M. Tavares, and M. M. Telo da Gama, *J. Phys.: Condens. Matter* **14**, 9171 (2002).
- [26] Z. Wang and C. Holm, *Phys. Rev. E* **68**, 041401 (2003).
- [27] J. J. Weis, *J. Phys.: Condens. Matter* **15**, S1471 (2003).
- [28] T. Kruse, A. Spanoudaki, and R. Pelster, *Phys. Rev. B* **68**, 054208 (2003).
- [29] H. Morimoto, T. Maekawa, and Y. Matsumoto, *Phys. Rev. E* **68**, 061505 (2003).
- [30] M. Aoshima and A. Satoh, *J. Colloid Interface Sci.* **280**, 83 (2004).
- [31] J. P. Huang, Z. W. Wang, and C. Holm, *Phys. Rev. E* **71**, 061203 (2005).
- [32] T. Kristóf and I. Szalai, *Phys. Rev. E* **72**, 041105 (2005).
- [33] J. M. Tavares, J. J. Weis, and M. M. Telo da Gama, *Phys. Rev. E* **73**, 041507 (2006).
- [34] P. D. Duncan and P. J. Camp, *Phys. Rev. Lett.* **97**, 107202 (2006).
- [35] J. J. Cerdà, S. Kantorovich, and C. Holm, *J. Phys.: Condens. Matter* **20**, 204125 (2008).
- [36] E. Pyanzina, S. Kantorovich, J. J. Cerdà, A. Ivanov, and C. Holm, *Mol. Phys.* **107**, 571 (2009).
- [37] M. I. Shliomis, *Sov. Phys. Usp.* **17**, 153 (1974).
- [38] A. Tsebers, *Magnetohydrodynamics (N.Y.)* **18**, 345 (1982).

- [39] A. F. Pshenichnikov, V. V. Mekhonoshin, and A. V. Lebedev, *J. Magn. Magn. Mater.* **161**, 94 (1996).
- [40] M. S. Wertheim, *J. Chem. Phys.* **55**, 4291 (1971).
- [41] K. I. Morozov, *Bull. Acad. Sci. USSR, Phys. Ser. (Engl. Transl.)* **51**, 32 (1987).
- [42] K. I. Morozov and A. V. Lebedev, *J. Magn. Magn. Mater.* **85**, 51 (1990).
- [43] G. S. Rushbrooke, G. Stell, and J. S. Hoye, *Mol. Phys.* **26**, 1199 (1973).
- [44] J. Wagner, B. Fischer, and T. Autenrieth, *J. Chem. Phys.* **124**, 114901 (2006).
- [45] I. Szalai and S. Dietrich, *J. Phys.: Condens. Matter* **20**, 204122 (2008).
- [46] Y. A. Buyevich and A. O. Ivanov, *Physica A* **190**, 276 (1992).
- [47] A. O. Ivanov, *Magnetohydrodynamics (N.Y.)* **28**, 39 (1992).
- [48] J. Wagner, B. Fischer, T. Autenrieth, and R. Hempelmann, *J. Phys.: Condens. Matter* **18**, S2697 (2006).
- [49] A. Wiedenmann, M. Kammel, A. Heinemann, and U. Keiderling, *J. Phys.: Condens. Matter* **18**, S2713 (2006).
- [50] L. M. Pop and S. Odenbach, *J. Phys.: Condens. Matter* **18**, S2785 (2006).
- [51] E. Elfimova and A. Ivanov, *Magnetohydrodynamics* **44**, 39 (2008).
- [52] Z. Wang, C. Holm, and H. W. Müller, *Phys. Rev. E* **66**, 021405 (2002).
- [53] J. D. Weeks, D. Chandler, and H. C. Andersen, *J. Chem. Phys.* **54**, 5237 (1971).
- [54] B. Groh and S. Dietrich, *Phys. Rev. Lett.* **79**, 749 (1997).
- [55] B. Groh and S. Dietrich, *Phys. Rev. E* **57**, 4535 (1998).
- [56] R. Balescu, *Equilibrium and Nonequilibrium Statistical Mechanics* (Wiley, New York, 1975).
- [57] M. S. Wertheim, *Phys. Rev. Lett.* **10**, 321 (1963).
- [58] J. Chang and S. I. Sandler, *Mol. Phys.* **81**, 735 (1994).
- [59] B. R. A. Nijboer and L. Van Hove, *Phys. Rev.* **85**, 777 (1952).
- [60] A. O. Ivanov and O. B. Kuznetsova, *Phys. Rev. E* **64**, 041405 (2001).
- [61] J. J. Cerdà, V. Ballenegger, O. Lenz, and C. Holm, *J. Chem. Phys.* **129**, 234104 (2008).
- [62] M. P. Allen and D. J. Tildesley, *Computer Simulation of Liquids* (Clarendon, Oxford, 1987).
- [63] H. J. Limbach, A. Arnold, B. A. Mann, and C. Holm, *Comput. Phys. Commun.* **174**, 704 (2006).
- [64] G. Mériguet, M. Jardat, and P. Turq, *J. Chem. Phys.* **121**, 6078 (2004).